東方宗教評論

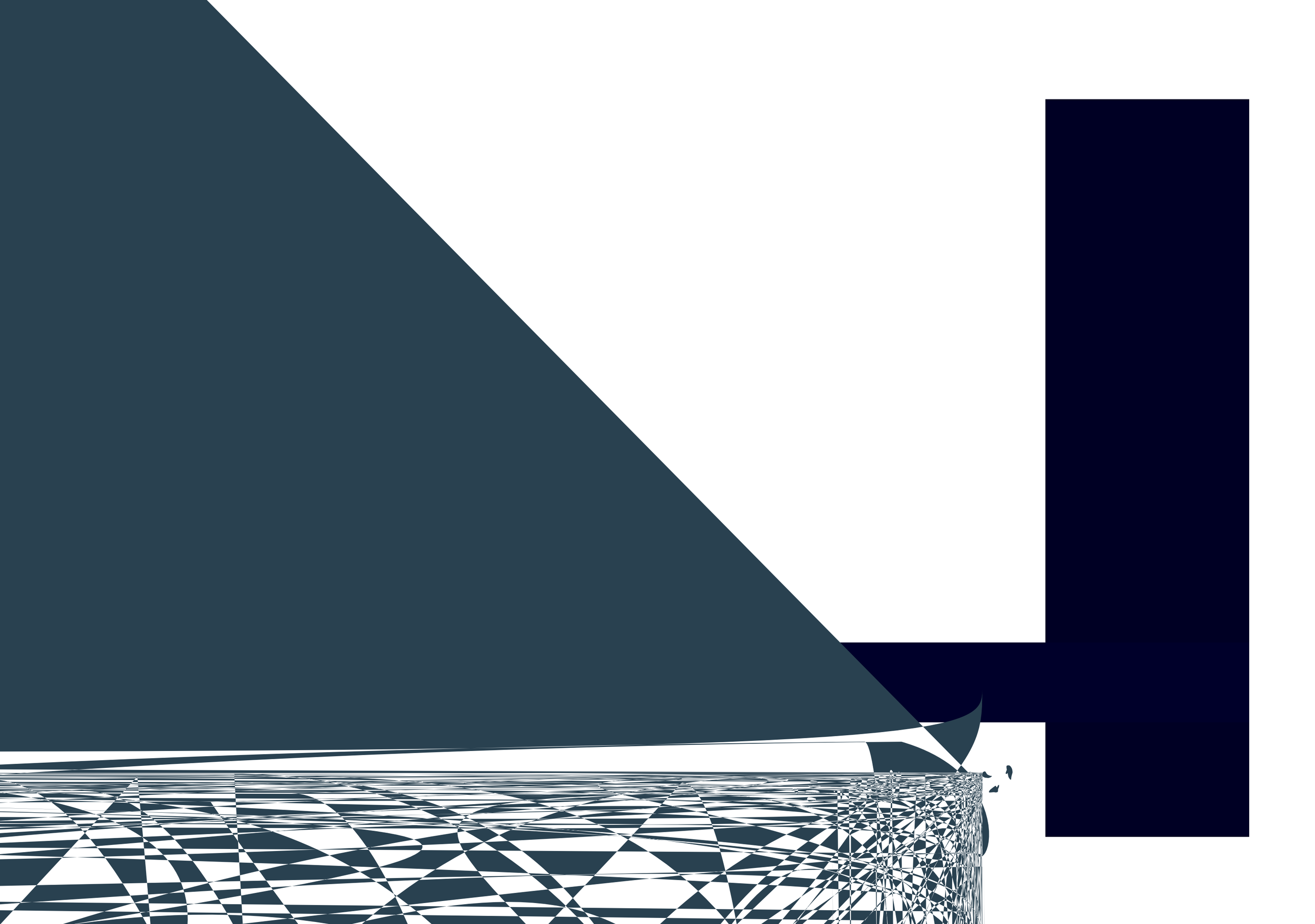

1 1 1 2 1

1. 611731 2. 618000

Functional Design and Application of Manufacturing Operation Management System for Digital Workshops in Large Boiler Equipment Manufacturing Industry

Abstract: Aiming at the production management requirements of large boiler equipment manufacturing enterprises during equipment development, a manufacturing operation management system covering the entire business process of the workshop was designed and applied. Through the design of modules such as the plan control center, plan management, material management, production execution, qualim ®nagem

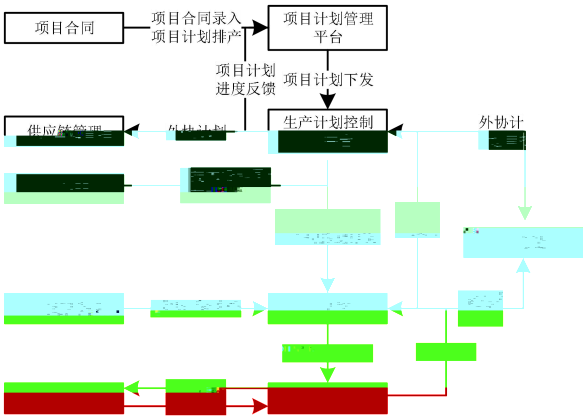
项目合同
项目合同录入
项目计划排产
项目计划管理平台
项目计划进度反馈
项目计划下发
供应链管理
生产计划控制
外协计

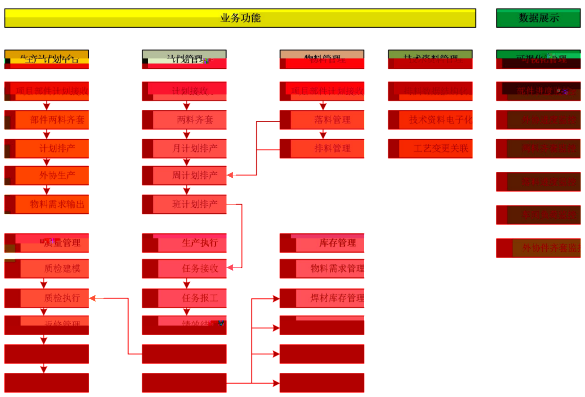
业务功能
数据展示

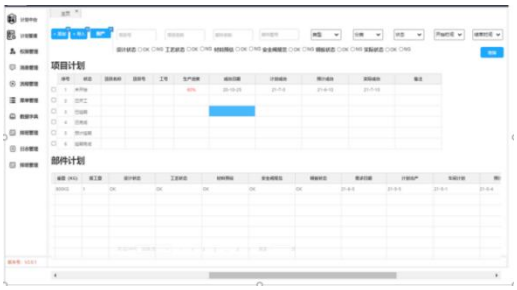
项目计划
部件计划

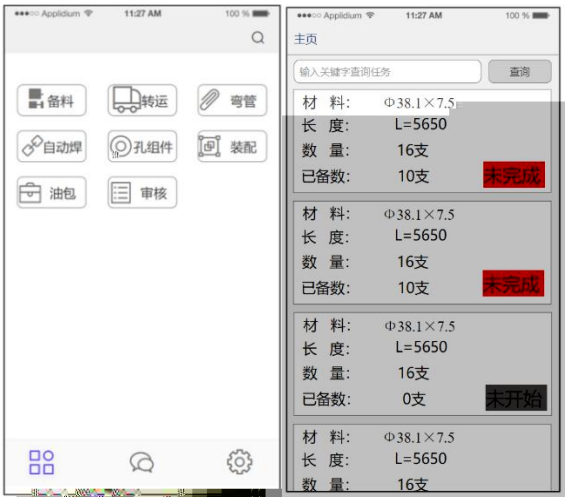
备料
转运
弯管
自动焊
孔组件
装配
油包
审核
主页
输入关键字查询任务
查询
材 料: Φ38.1×7.5
长 度: L=5650
数 量: 16支
已备数: 10支
未完成
材 料: Φ38.1×7.5
长 度: L=5650
数 量: 16支
已备数: 10支
未完成
材 料: Φ38.1×7.5
长 度: L=5650
数 量: 16支
已备数: 0支
未开始
材 料: Φ38.1×7.5
长 度: L=5650
数 量: 16支

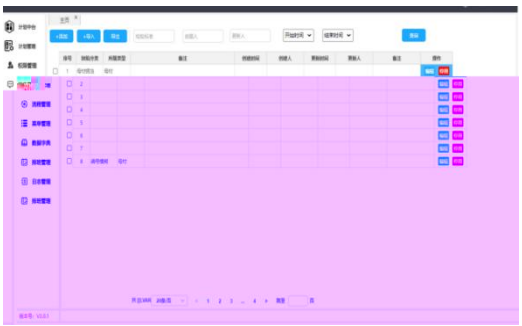

PLM CAPP CAPP

MOM

,

,

:

:

,

:

,

:

,

,

,

,

,

,

BOM

1 2 2 1 1

1. 611731 2. 643000

T5 BOM BOM

MOM

T5 BOM

TK222 A 1001-9006 2023 02-0006-04

J GS V 1, U L E J 2, J G W 2, GL E H 1, W GL O 1

(1. Dec Academy of Science and Technology Co., Ltd., 611731, Chengdu, China; 2. Dongfang Boiler Co., Ltd., 643000, Zigong, Sichuan, China)

2025 CAPP ERP MOM

/ @MK ⅞

2023

84%

2023-04-14

SC0021044

(2000) 2022

[1] A

BOM

A A

T5 1

T5

MOM

MOM

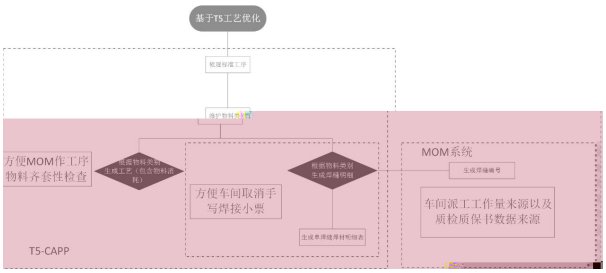

1 T5

0 ? Å ˝ @MK ↄ ⅞

2.1 BOM

2.1.1 BOM

BOM

BOM

material>3, 3

2.1.2

2

3

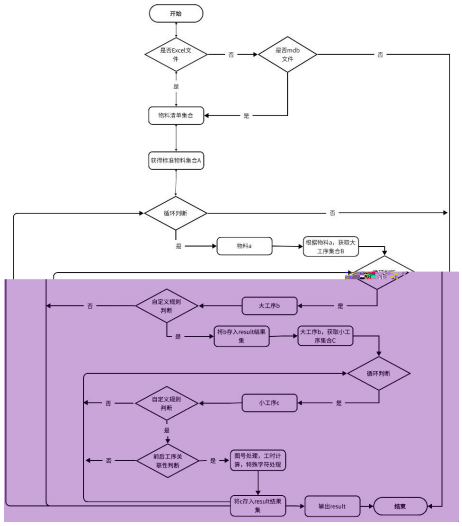

2

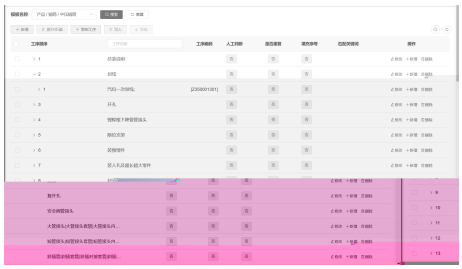

3

2.2 BOM

2.2.1

A+ B=>

A

A A18

A 18

x/y x/z

x y x/y-z x/y-n x,y,z,n

x/y

x/y-z

C 3/4-1, 3/4-x

3/x

A

B C A B

C

2.2.2

$M=N=\{a,b,c,d,...\}$ i

$P=\{A=\{1,x,a,b,0\}, B=\{2,y,c,c,1\},$

$C=\{3,z,a,b,0,1\}, D=\{4,h,b,c,d\},...\}$

j A

x a b 0

0 B 1 0

C 0 1

D

R

2.2.3

M P N P M, P N

Z $P.Z=M\times N$

1 M P N 4

M P N

m^2p

O n^3

$U=\{X|X=P_p-M_m, M_m\in P_p, m\in 1,2,3,...,i, p\in 1,2,3,...,j\}$

$V=\{Y|Y=U_u-N_n, N_n\in U_u, n\in 1,2,3,...i, u\in 1,2,3,...,x\}$

$R=\{r|r=P_p, V_v\subseteq P_p, p\in 1,2,3,...,j, v\in 1,2,3,...,x\}$

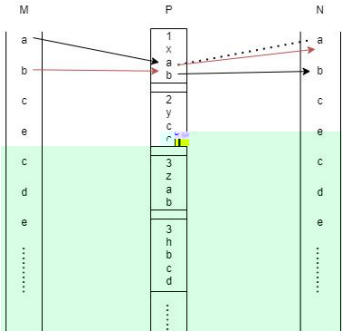

4 M-P-N

2 P M, P N 5

P M N

mp $O(n^2)$

$R=\{r|r=P_p, M_m\in P_p, N_n\in P_p, m,n\in 1,2,3,...,i, p\in 1,2,3,...,j\}$

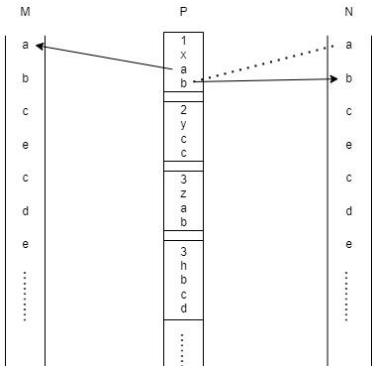

5 P-M,P-N

3 Z P $Z=M\times N$ 6

M N

Z M N P

M N

m^2 $O(n^25$

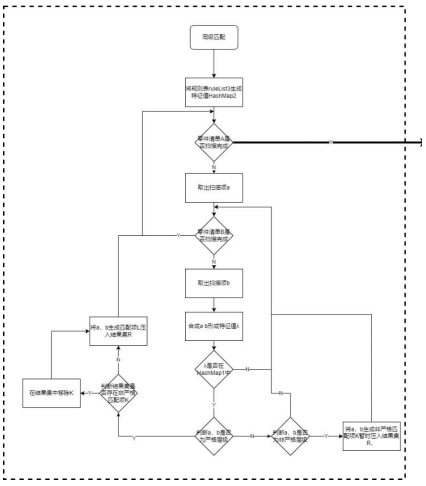

8

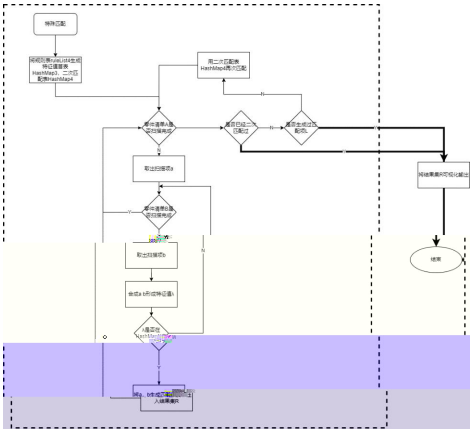

9

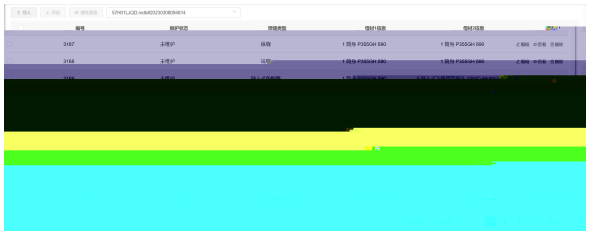

10

1 ↄ ⅞

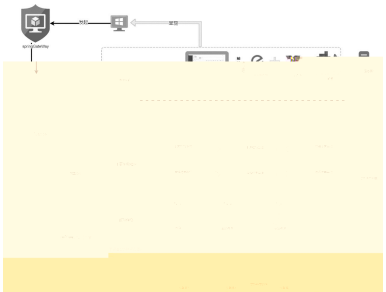

11

11

T5

MOM

2

BOM

A T5

1

70%

2

30%

3 MOM

4

MOM

AI BOM

[1] , . 2022 [R]. , , 2023-1-11

[2] , , . BOM [J]. , 2003(8):42-44

[3] . [R/OL].https://developer.aliyun.com/topic/cn-architecture-paper

[4] , , . BOM [J]. , 2007(4):43-47

[5] , , . BOM [P]. CN113569107A,2021-10-29

M701F4 — APS “ ”

“ ”

Automatic Plant Startup and Shutdown System Development and Application of Mitsubishi M701F4 Gas Combined Cycle Unit

CHEN Qi, YAN Jindong, LONG Tao

Abstract: As a two-shift peak-shaving operation unit, the realization of "one-key start and stop" (Automatic Plant Startup and Shutdown System, APS) is of great significance to standardize the control and operation of the unit start and stop process. This project has carried out in-depth research on the start-up and shutdown process of Mitsubishi M701F4 combined cycle unit, developed the configuration and verification of the unit APS control logic, optimized and improved the unreasonable part of the original control logic, realized the effective control and regulation of the APS function module on the unit's various equipment, and significantly improved the safety and economy of the unit in the start-up and shutdown stage.

Key words: APS; start and stop; shakedown test; optimize

1 APS

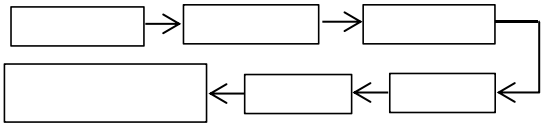

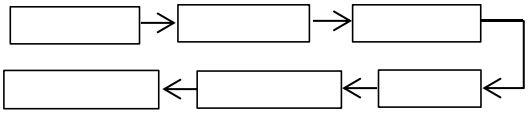

3

2 APS

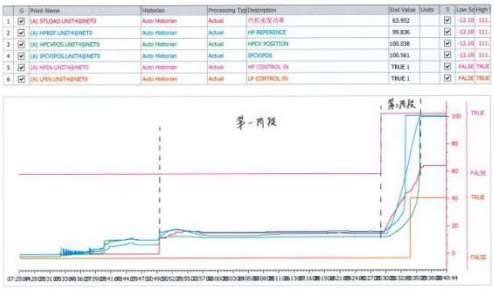

	G	Pnvt Name	Historian	Processing Typ	Description	End Value	Units	S	Low Sc	High
1	☑	(A) ST LOAD.UNIT4@NET0	Auto Historian	Actual	汽机实发功率	63.952		☑	-12.05	111.
2	☑	(A) HPREF.UNIT4@NET0	Auto Historian	Actual	HP REFERENCE	99.836		☑	-12.05	111.
3	☑	(A) HPCVPOS.UNIT4@NET0	Auto Historian	Actual	HPCV POSITION	100.038		☑	-12.05	111.
4	☑	(A) IPCVSPOS.UNIT4@NET0	Auto Historian	Actual	IPCVSPOS	100.561		☑	-12.05	111.
5	☑	(A) HPEN.UNIT4@NET0	Auto Historian	Actual	HP CONTROL EN	TRUE 1		☑	FALSE	TRUE
6	☑	(A) LPEN.UNIT4@NET0	Auto Historian	Actual	LP CONTROL EN	TRUE 1		☑	FALSE	TRUE

4 APS

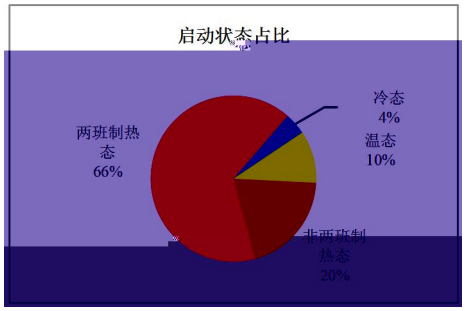
启动状态占比
冷态
4%
温态
10%
两班制热态
66%
非两班制热态
20%


#4机两班制热态启动数据
项目启动前
逻辑优化阶段
APS 调试阶段
成本
启动耗时
150.00
140.00
130.00
120.00
110.00
100.00
90.00
80.00
12
11
10
9
8
7
6
2018/9/19
2018/9/29
2018/10/12
2018/11/13
2018/11/29
2018/12/19
2019/3/12
2019/3/23
2019/3/26
2019/3/29
2019/4/3
2019/4/9
2019/4/18
2019/4/26
2019/6/5
2019/6/26
2019/7/27
2019/8/13

/ 3 .

0 . 0 1 3 /

/ 3 .

“ ”

“ ”

/ 3 .

“ ”

/ 3 .

“ ”

“ ”

/ 3 .

/ 3 .

“ ”
. /

/ 3 .

/ 3 .

0 . 2

CN51-1333/TM

ISSN1001-9006

(GB/T7713.2—2022) GB7714

“ ”

1

2

3

4

5

6

7

8

9

10

11

18650

611731

/ 0 0 .

1 2

/ . . / + . . 0 . 0 1 . 0 +. . / +. 2

ZHU Rui ZHANG Zhongwei WANG Jing LIAO Xiaodong

& . . / / 1 / '

( ) ( )

( )

( )

0 / 3 . .

/ +0

1 +/

/ +0 0

1

/ , /

+ +

0 . 0 1 +. 1 +0 .

/ 0 . / 0

/ ,0

/ ,0 , /

+

2 ,3 # 0 # 0 #

/ ,3 #

+

3 # 1 # 0 #

/ 3 . / 3 .

3 0 2

/ ,0 ,0

3 . # 1 . # 0 . #

/

/

	#
/	/ .
0	/ 0

/ ,0 ,1

/ ,0

/ 3 .

2

0 , /

/ . . .

. 2 2

3 . .

3 . .

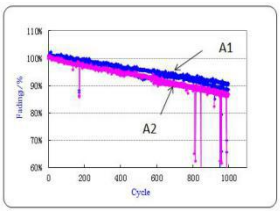

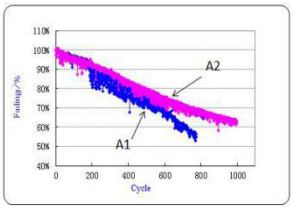

,0 3 2 -2 , . 2 -2

/

0 ,0

0

0

#					
/	1	3	/ .	0 .	
/	/ . . ,. .	3 ,2 /	3 ,0 1	,. 3	. ,. 0
0	/ . . ,. .	2 , .	2 , 3	3 , .	,1 .

/ 1 3 / . 0 .

/ . ,3 0 3 3 ,1 / . ,/ 1 0 2 2 1 ,.

0 . ,/ 2 ,0 ,2 0 . , 3 2 . ,/

/ 1 3 / .

0 .

#

0 ,1

1

#

/ 1 3 / .

/ / . . ,. . / . 0 , / . / , ,0 ,

0 / . . ,. . / . 1 ,1 / . 0 , / . . ,0 . ,

/ 1 3 / .

/ / ,0 ,0 / 0 / , 0 1 ,

0 / , ,3 / 1 ,/ / ,1 0 1 ,3

1 /

/ .

1 3 / . . #

/ 1 3

/ 0 # 1 #

0 ,2

/ . / . / .

3 . #

/ . . - / 3 .

/ 2 . . -

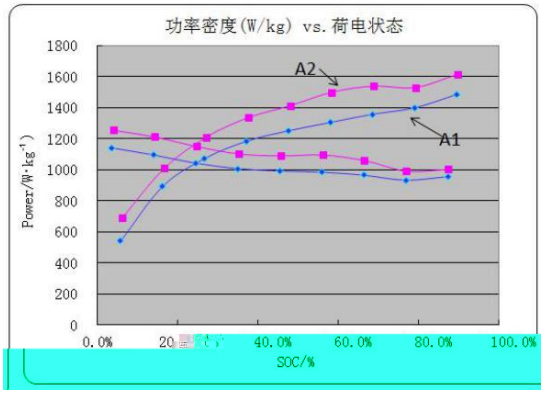

0

0 ,3

0 3

2

2

#

+/ . . / . 0 3 2 3 .

/ . ,2 3 / ,/ ,. 0 / . . ,. . / . / ,. / . / ,1 1

0 3 , 0 , , / . . ,. . / . / ,/ 2 / . / ,2 0

3

20C

[1] . [J]. , 2011, 35(1):12-14

[2] , , . - [M]. : , 2004

[3] , , . [J]. , 2007(S1):267-269

[4] , , . [J]. , 1998(2):47-50

[5] . [D]. 2022

[6] , , . [J]. , 2004(2):89-91

[7] Huang Shahua Wen Zhaoyin Yang Xuelin et a1. Improvement of the high-rate discharge properties of LiC002 with the Ag additives[J]. J Power Sourc, 2005(148):72

[8] Christine A Frysz Shui Xiaoping Chung D D L Carbon filaments and carbon black as a conductive additive to the manganese dioxide cathode of a lithium electrolytic cell[J]. J. Power Source, 1996 (58):41

[9] Cheon S E, Kwon C W, Kim D B, et a1. Effect of binary conductive agents in LiCoO2 cathode on performances of lithium ion polymer battery[J]. Electrochim Acta, 2000(46):599

[10] Li Xinlu, Kang Feiyu, Shen Wanci. Multiwalled carbon nanotubes as a conducting additive in a LiNi0. 7 Coo. 3 02 cathode for rechargeable lithium batteries[J]. Carbon, 2006(44):1298

[11] Ahn Soonho, Kim Youngduk, Kim Kyung Joon, et a1. Development of high capacity, high rate lithium ion batteries utilizing metal fiber conductive additives[J]. J Power Source, 1999(81-82):896

[12] . [J]. , 2005(2):78-79+91

[13] Liu Zhaolin, Lee Jim Y, Lindner H J. Effect of conducting carbon on the electrochemical performance of LiCoO2 and LiMn204 cathodes[J]. J Power Source, 2001(97-98):361

[14] Hong Jin K, Lee Jong H, Oh Seung M Effect of carbon additive on electrochemical performance of LiCoO2 composite cathodes[J]. J Power Source, 2002(111):90

[15] Shui Xiaoping, Frysz C A, Chung D D L. Solvent cleansing of the surface of carbon filaments and its benefit to the electrochemical behavior[J]. Carbon, 1995, 33(12):1681

[16] Frysz C A, Chung DD L. Improving the electrochemical behavior of carbon black and carbon filaments by oxidation[J]. Carbon, 1997, 35(8):1111

[17] , , . [J]. , 2003(9):34-37

[18] , , . [J]. , 2004(3):57-60+71

[19] , , . [J]. , 2008(1):68-71

[20] , . [J]. , 2000(1):116-118

[21] , , . [J]. , 2001(2):91-93

[22] , , . SEI [J]. , 2002(6):354-357

1,2 **1,2** **1,2** **1,2** **1,2**

1. 610005 2. 610005

TM623 A 1001-9006 2023 02-0023-04

LONG Tao[1,2], *WEN Xiaojun*[1,2], *DING Ran*[1,2], *LIU Jian*[1,2], *HU Hongxing*[1,2]

(1. Nuclear Power Institute of China, 610005, Chengdu, China;

2. Sichuan Engineering Laboratory for Nuclear Facilities Decommissioning and Rad-Waste Management, 610005, Chengdu, China)

,

,

,

,

,

,

,

,

,

,

,

,

2023-04-10

1988 2015

[1-3]

[4]

[5]

[6]

[7-8]

[redacted]

Marcore

1.204 Marcore

Marcore

llOS- DMS

4 5

4

5

4

[1] , , . [J]. , 2020,37(7):75-78

[2] . [D]. , 2013

[3] , , . [J]. , 1997(1):43-45

[4] , , . [J]. , 2020(8): 61-62

[5] , , . [J]. , 2018(11):39-43

[6] . . , , 2017-06-16

[7] , . [J]. , 2013(27):68-69

[8] . [J]. , 2017(18):89-91

[9] . [D]. , 2017

2023 3 17

CFR600

) 511455

Key Welding Technology of CFR600 Demonstration Fast Breeder Reactor Steam Generator

DAN Jun LI En JIANG Yuchen DENG Daoyong DAI Guangming

Abstract: CFR600 demonstration fast breeder reactor steam generator is the fourth Nuclear reactor designed by China.In this paper, the structural characteristics, the welding materials and the requirements of CFR600 steam generator was described. Meanwhile, the key welding processes to be implemented, such as the tube-to-tube sheet weld, Joint technology of sodium inlet and outlet pipe and heat-resistant stainless steel dissimilar steel, technology of dissimilar metal docking between chromium molybdenum steel (F22) and F91 material, ring joint technology of extra-large wall thick chromium molybdenum steel, have been introduced in detail, which provides technical supports for the design and development of the fourth generation nuclear power reactor steam generator.

Key words: fast breeder reactor; nuclear power technology; steam generator; welding technology

ج ǐ × ∪ ر

× ×

1

ŭ ر

ŭ ر ŭ ر´ Ƈ ŭ ر غ ر ŭ

ر غ ر ٥ ۔

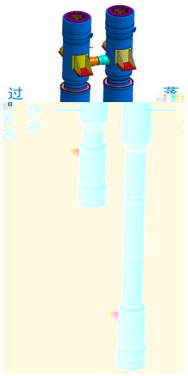

ŭ ر ×

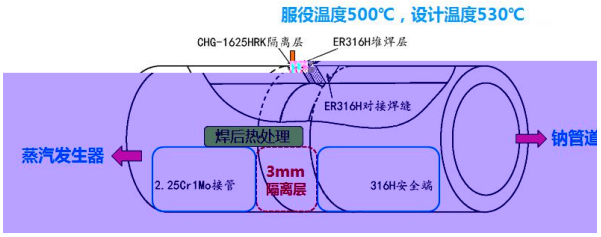
服役温度500℃，设计温度530℃
CHG-1625HRK隔离层
ER316H堆焊层
ER316H对接焊缝
焊后热处理
蒸汽发生器
钠管道
2.25Cr1Mo接管
3mm
隔离层
316H安全端

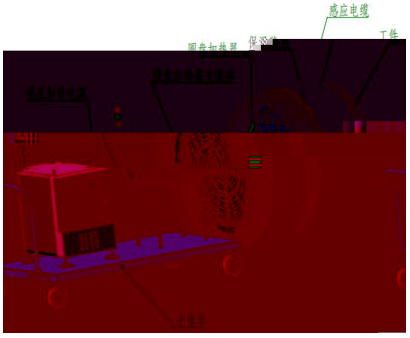
感应电缆

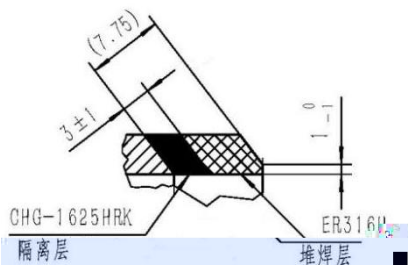
(7.75)
3±1
CHG-1625HRK
ER316H
隔离层
堆焊层

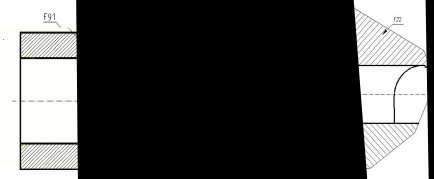

8 F22

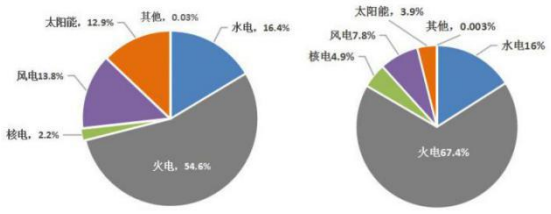

(a) (b)

1 2021

/ 2021 2022 3 2022 3 600 3 830 3 000 1 300 1 800 [1]

1 280 MW 850 MW 240 MW 48 MW 2 MW 12.8 MW 15.2 MWh [2] 1 200 MW 7.7%[3]

1

2030 2060 3.8 1 1 1 3 600 1 280 MW 850 MW 240 MW 48 MW 2 MW 12.8 MW 15.2 MWh 1 200 MW 7.7%

1

		0.12	
		0.24	
		1.3	86%
		2 281	
		1 080	
		500	
		3 100	2 043

ê Ч ج غ Ψ
Ď Ч ضم ۞ Л ⅞ غ Ни 500’ Ч
ۜ Л Ì ’ Ч

ê “Ч ضم Л” Ď 450’ Ч
⅞ Ì ^ 3 000’ Ч ~ à

1 ⌟ à à ۞ ₋ Ď˘
1 000 ⌟ . Ď ˘ ج
ض Â

3’ Ч
۞ Ǝ 4 580 Ч
⌟ 1 650
807’ Ч

¨ غ à Ч à ▯ à ĭ ۞Ũ Ш r. Â
ǎ àŨ Ѧ Ч ▯ Ď˘ ʒ Л“Ч ضم Л”
100’ Ч Ũ Ѧ Â

Â

ضي ۞ ˘ Ί п
ʒ˘ Ί r ضي à àНu
à à Ω¨ Â ê Ţ
Ď ⅞ 2021-2035 ~ Ì˘ 2021 8 ˘
´ ĸ ʟ ı ^ Ч 300 MW˜ à ı
^ Ч 375 MW˜ à ^ Ч 300 MW˜ à
^ 350 MW˜ ضي ṕ˘ ج ₀₀
3 249’ Ч ˘ ضي Ч 5 513’ Ч ˘
څ Ч Ƃ Ш Â ⌡ 2025 ˘ ₀₀
ф 6 200’ Ч ˘ 2030 ˘ ì ₀₀ ’P

Â

ض Ч غ ʒ ⅞ ˘ Ч
U ۞ ε ʒ ২ طه Â

2.

2.1 .

ضي ۞ Ũ ε ˘ Ų ʒ ⁂
فج à Ţ ج ⅞ فج à ج ˘ ضي څ
˜ ˘ 2 4ž Â Ч ц
Ţ ففم Ч ۞ ˘ ج ض غ L
à۞ Ǝ ˘ ʒ G ۞ Ũ Ш r. Ď Â

2 /

1	Ε Ч “ ۞ Ũ Ш r. ” ض	300’ Ч	⅞
2	2GW“ ۞ Ũ ”	300MW à 1.2 GW à ۞ Ǝ 500 MW	ĸ ʒ Ь Ч ˘ 110 .
3	Ч ă ۞ Ũ ε	3 ۞ ă3 ۞ ۞ Ǝ à ˘ Ţ ج Ь ă Ď 1 100 MW	Ч ˘ 55 .
4	´ ۞ Ũ Ш r.	/	⁂ فج Ь´ ₀₀ Ъ Ч
5	ض	10 GW ۞ Ǝ +10 GW	Ч ˘ ⅞ Ţ
6	Ч ج“№ ۞ Ǝ Ь ε ₀₀ Ď ĭ ”	54 MW à 5 MW	Ţ ج ˘ Ţ
7	’ Ч’ ۞ Ш r. ض	300’ Ч ⁂˘ ۞ Ǝ 240’ Ч ⁂˘ 20’ Ч ⁂˘ 20 ’ Ч ⁂	Ď Ч ˘ 150 .

ضي ⅞ Ţ Ꮒ ˇ ڏ U ۏ
ε Â ˇ ضي
Ţˇ à И Ⴝ
ڏ Â

2.2.2

ۏ ε ╠. ɢ ˇ ч Ḡ
U r à ŭ à ε ᴡ ˇ
ˇ ۏ ₩ r. ’ И
ˍ ˇ ŭ

Ⲏ Â
ضي ٦ ˇ ٦ Ї
r ضيˇ Ŵ ŋ ’ ˇ №
څ ŋ ˇ Ỉ φ ŋ
’ Ŷ ڏ ˍ ’ ŷ
ˇ Ї ᴪ п ʒ ˇ ⅄ ʒ ˍ ’
Ÿ ɢ Ω Å à Ї˗ à
à ˇ Ꮄ Ї п
ė ˈ ʒ’ Ź ŭ Ї Ỉ
⅄ à ˍ ʒˇ ė
Â

ضي ˇ ضي h à
Ї Ї h ŭ Â ېج ɢ
Ϭ 60 ٹ . ⅄ ˇ à Ⴝ
à ښس ˇ ϶ ېج
ˇ ĸ ضي ᴸ Ţ شخ ă Ьˇ
╠ شي Ⅵ ŋ ېج ₩ Â ╠ˇ ېج ṗ
ضي 600 Ї ү И à ˇ ү
ĸ ч ٹ ° ჟˇ ېج ۏ ˇ
h Ї à№ à
h Â

2.2.3

ضي ۏ ... ˇ Ỉ h Ţ ضي
ۏ à ۏ ŭ Ь à ۏ
٧ Là ۏ ٧ [6] Â
ˍ [7] ۏ ε Ţ Ь ŋ
ˇ ă - -ŋ ŭ à
ŭ Ḡ ė ٧ Â ₩ ˍ [8]
... ۏ Ǝ ∓ ʒ ڤ ė ۏ ڤˇ
٧ ۏ ė Â à ۏ Ǝ ∓ ʒ
... Ţ ₩ ˇ ۏ ∓ ʒ ضي
ل ˇ ېج 2 ˇ Ỉ ˇ

Â [9] ˇ ү ۏ
ε ’ ŭ ˇ Ь à Ь
ð И Ь ڤˇ ∓ ʒ
‰ Â

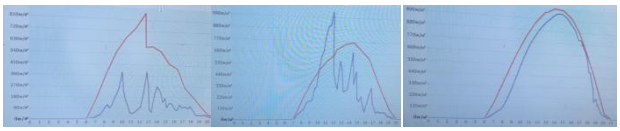

(a) (b)

2

2.2.4

ˍ [10] № à № ė
Shapley ỵ № ˇ ۏ Ǝ
ɔ ƶ ẁ h ă Ь ε ˇ ң ˇ Ꝑ ң Â

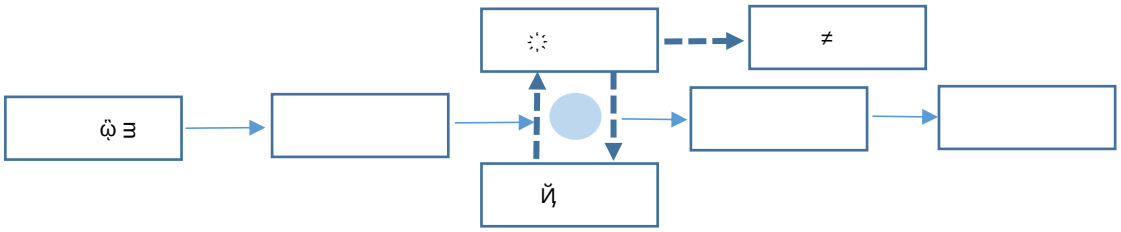

3 - - -

4

[1] , , . [J]. , , 2016,35(3):105-108

[2] , , , . [J]. , 2020, 35(13):2711-2722

[3] , , , . [J]. №, 2020,5(2):21-26

[4] Xu Xiao, Hu Weihao, Cao Di, et al. Optimized sizing of a standalone PV-wind-hydropower station with pumped-storage installation hybrid energy system[J]. Renewable Energy, 2020, 147: 1418-1431

[5] , , . [J]. , 2020(10):130-134

[6] , , , . [J]. , 2022,42(11):3871-3885

[7] , , , . [J]. , 2021,7(5):20-24

[8] , , , . [J]. , 2020,38(10):207-210+106

[9] . [J]. , 2020(1):23-26

[10] , , , . [J]. №, 2022,22(10):3991-3997

[11] , , , . [J]. , 2021, 44(4):67-71

[12] , , , . [J]. №, 2020, 52(3):32-41

[13] , , , . [J]. , 2020,18(6):494-501

618000

4

:

TM315 A 1001-9006 2023 02-0036-05

Comparison of Parameter Estimation Methods for Extreme Load Extrapolation of Wind Turbine

WANG Jun, YIN Jingxun, ZHAO Wei, ZENG Qingzhong

(Dongfang Electric Wind Power Co., Ltd., 618000, Deyang, Sichuan, China)

Abstract: In this paper, the global maximum method is used to extract the maximum load from each simulation of wind turbine, and the three parameter Weibull distribution is used to predict long-term extreme load. The extrapolation results of four parameter estimation methods including L-moment estimation, correlation coefficient estimation, maximum likelihood estimation and moment estimation are compared.

Key words: extreme load extrapolati o a aa wepoh eip

- -

IEC

1.4

[3]

[4]

[5]

1.2

n

$x_1 \leqslant x_2 \leqslant \ldots \leqslant x_n$

$$F_{\text{short-term}} \quad x \quad \frac{i}{n \quad 1}, i \quad 1, \quad , n \qquad 1$$

$$F \quad x \quad 1 \quad exp \quad \frac{x}{\qquad} \qquad 2$$

γ— η— β—

1.3

N $V_1 \leqslant V_2 \leqslant \ldots \leqslant V_N$

$$F_{\text{long-term}} \quad x \quad \sum_{k \quad 1}^{N} F_{\text{short-term}} \quad (x \mid V_k) P_k \qquad 3$$

10 50

$10/(50\times365.25\times24\times60)= 3.8\times10^{-7}$ P_k

10

$$P \quad V \quad 1 \quad exp \quad \pi \quad V / 2V_{\text{ave}}{}^{2} \qquad 4$$

V_{ave} 10

2

2.1 [6]

1 0

2 2 1 0

3 6 2 6 1 0

4 20 3 30 2 12 1 0 5

r

$$\frac{1}{0} \quad \frac{1}{n} \sum_{i \quad 1}^{n} x_i \qquad 6$$

$$\frac{1}{r} \quad \frac{1}{n} \sum_{i \quad 1}^{n} \frac{(i \quad 1)(i \quad 2)\cdots(i \quad r)}{(n \quad 1)(n \quad 2)\cdots(n \quad r)} x_i, r \geq 1$$

$$r \quad \frac{r}{2}, r \quad 2 \qquad 7$$

$$\frac{\log(2)}{\log(\frac{5}{4 \quad 5 \quad 3 \quad 4})} \qquad 8$$

$$1 \quad \frac{5 \quad 2}{4 \quad 5 \quad 3 \quad 1} \qquad 9$$

$$(\quad 1 \quad) / \quad \frac{\log(\frac{10}{4 \quad 5 \quad 3 \quad 4})}{\log(2)} \qquad 10$$

2.2 [7]

2

$$\text{In} \quad \text{In} \quad 1 \quad F \quad x \quad \text{In} \quad x \quad \text{In} \qquad 11$$

:

$$Y \quad \text{In} \quad \text{In} \quad 1 \quad F \quad x$$

$$X \quad \text{In}(x \quad)$$

$$A \qquad 12$$

$$B \quad \text{In}$$

12

$$Y \quad AX \quad B \qquad 13$$

12

X_i, Y_i A B

$$A \quad \frac{\sum_{i \quad 1}^{n} X_i Y_i \quad (\sum_{i \quad 1}^{n} X_i \sum_{i \quad 1}^{n} Y_i) / n}{\sum_{i \quad 1}^{n} X_i^2 \quad (\sum_{i \quad 1}^{n} X_i)^2 / n} \qquad 14$$

$$B \quad \sum_{i \quad 1}^{n} Y_i / n \quad A \sum_{i \quad 1}^{n} X_i / n$$

X Y R

$$R=\frac{(\sum_{i=1}^{n}X_iY_i-(\sum_{i=1}^{n}X_i)(\sum_{i=1}^{n}Y_i)/n)^2}{(\sum_{i=1}^{n}X_i^2-(\sum_{i=1}^{n}X_i)^2/n)(\sum_{i=1}^{n}Y_i^2-(\sum_{i=1}^{n}Y_i)^2/n)} \quad 15$$

15 R η 12 γ β

2.3 [8]

$\ln L(x_1,\ldots,x_n;\ ,\ ,\ n\ln\ n\ln$

$$1\sum_{i=1}^{n}\ln x_i\quad\frac{1}{}\sum_{i=1}^{n}x_i \quad 16$$

8 η 0

$$\frac{1}{n}\sum_{i=1}^{n}x_i \quad 17$$

9 8

$\ln L(x_1,\ldots,x_n;\ ,\ n\ln\ n\ n\ln\ n$

$$1\sum_{i=1}^{n}\ln x_i\quad n\ln\sum_{i=1}^{n}x_i \quad 18$$

18

γ β

9 η

2.4 [9]

$g_i(\ )\quad(1\ \ i/\ ),i\ \ 1,2,3$

$E(x)$ $\sigma(x)$ $B(x)$

$\overline{X}$ S B

$E(x)\quad g_1(\ )$ (19)

$x\quad\sqrt{g_2(\ )\ \ g_1^2(\ )}$ (20)

$$B\ x\quad\frac{g_3(\ )\ \ 3g_2(\ )g_1(\ )\ \ 2g_1^3(\ )}{[g_2(\ )\ \ g_1^2(\ )]^{3/2}} \quad (21)$$

$$\overline{X}\quad\frac{1}{n}\sum_{i=1}^{n}x_i \quad (22)$$

$$S\quad\sqrt{\frac{1}{n\ \ 1}\sum_{i=1}^{n}(x_i\ \ \overline{X})^2} \quad (23)$$

$$B\quad\frac{n}{(n\ \ 1)(n\ \ 2)S^3}\sum_{i=1}^{n}(x_i\ \ \overline{X})^3 \quad (24)$$

η γ β

3

GH Bladed Kaimal

DLC1.1 10 2 m/s 9

Mx 1 My 2 3

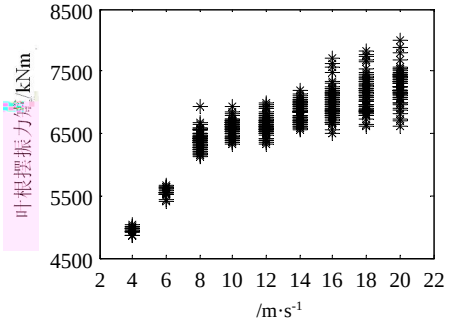

1 Mx

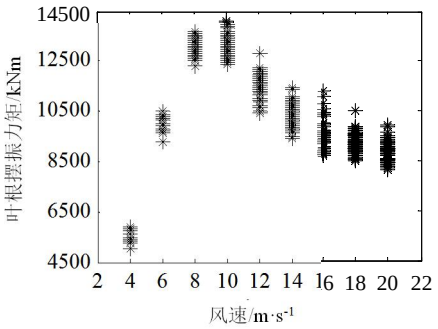

2 My

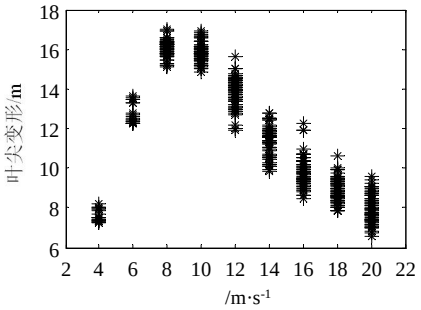

3

IEC 15 2 m/s 6 [10]

18 60 10 1

0.295	18
	18
	60

4

< 5 m/s 5 7 m/s 13 15 m/s 17 19 m/s

9 11 m/s 11 13 m/s

3

7 9 m/s 15 17 m/s >19 m/s

4

5 15 17 m/s

4

4

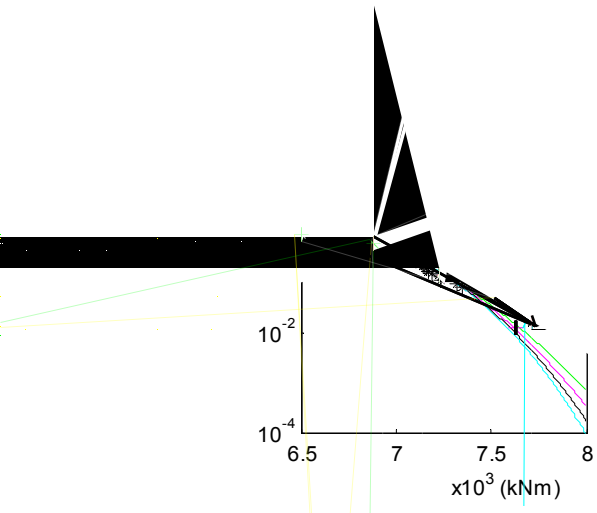

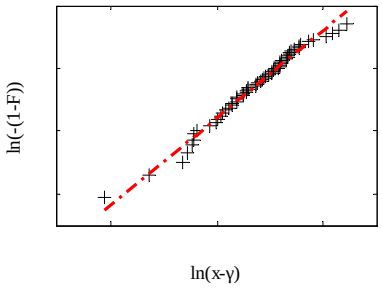

5

3.2

3

50

6 7 8 2

4

2 50

	Mx	My	
	1.080	1.122	1.056
	1.058	1.106	1.030
	1.070	1.123	1.055
	1.067	1.111	1.055

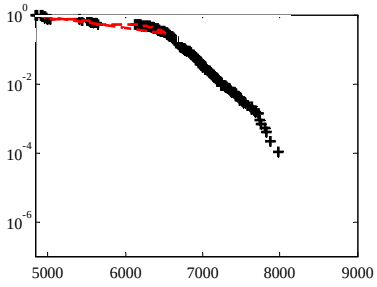

1 1 1* 1 2

TM615 A 1001-9006 2023 02-0041-07

Research Progress on the Software of the Heliostat Field Layout of the Solar Tower Thermal Power Plant

HUANG Ju, *YAN Zhiguo*, *DENG Biao**, *WANG Zhiming*[1], *ZHU Tong*[2]

(1. Dongfang Electric Automation Control Engineering Co., Ltd., 610036, Chengdu, China;

2. School of Mechanical Engineering, Tongji University, 201804, Shanghai, China)

Abstract: During the "Fourteenth Five-Year Plan" period, the four-dimensional integration and multi-energy complementation of solar and thermal storage will be the new trend of energy utilization, and tower solar thermal power generation will usher in new development with its own advantages. However, with the increase of the capacity of the mirror field in the photothermal power station, the problems of high computational cost and low efficiency of the existing mirror field design software are increasingly prominent. This paper introduces and summarizes the key algorithms in those softwares, such as initial layout, efficiency calculation, layout optimization, energy flow density distribution of the receiver, analyzes the differences in functions and algorithms of different software.At last,the existing problems and some suggestions of the development of the software are discussed ,and an outlook on the future development for the next research has been prospected.

Key words: solar tower thermal power; mirror field layout; design software; algorithms

“ ”

?Ø7-3+

“ ”

2023-02-20

1982 2008

1991 1094153808@qq.com

SolarPilot

SPD100 HFLD

60 %

28 % 12 %

50 SolTrace Tonatiuh

TieSOL SPD100

1.98 GPU

1

40-50 %[2]

RECEL	1977	√	√		√	√	√		[3]
MIRVAL	1979		√			√		√	[4]
DELSOL3	1986	√	√	√		√	√		[5]
UNIZAR	1989		√	√		√	√		[6]
SolTrace	2003		√			√		√	[7]
Tonatiuh	2005		√			√		√	[8]
HFLD	2006	√	√			√		√	[9]
HFLCAL	2009	√	√			√	√		[10]
TieSOL	2011	√	√			√		√	[11]
Campo	2012	√	√			√			[12]
SolarPilot	2018	√	√	√	√	√	√	√	[13]
SPD100	2019	√	√	√	√	√	√	√	[14]

2.1

1

1

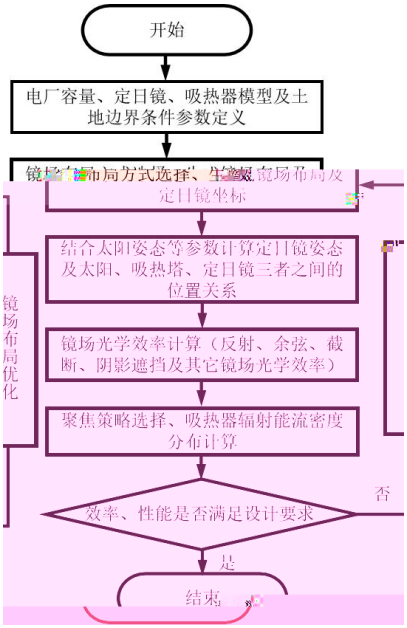

1

2.2

[15]

2

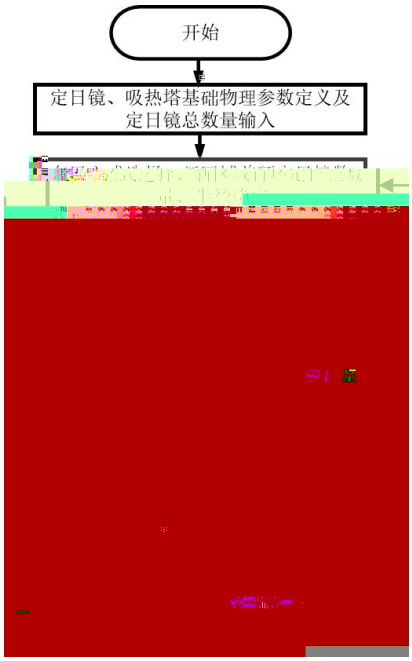

2

2.2.1

3

Campo

[12]

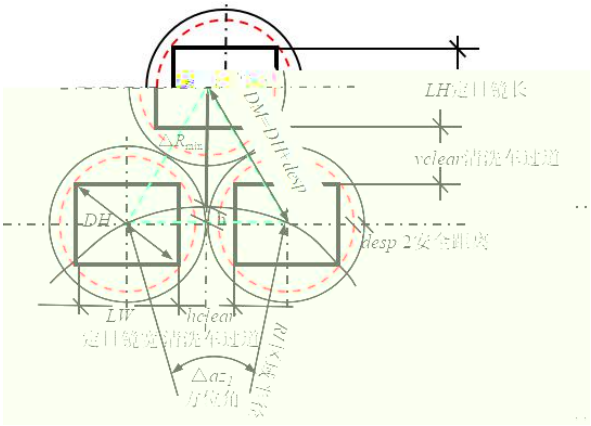

3 Campo

2.2.2

Confield layout

Radial Staggered Layout

Biomimetic layout Variable and Un-Even heliostat fields 4

Lipps Vant-Hull [3] 1978

4a b

4c

1986 DELSOL3 [5]

Lipps Walzel [3,16]

[17]

4d

[3]

[12]

Campo

4e

Campo [18] 2.3

1 “ a ” “ b ”

4f

[19]

$$r = ak^b$$
$$\theta = 2\pi\varphi^{-2}k$$

1

r θ φ

$\frac{1+\sqrt{5}}{2}$ a b

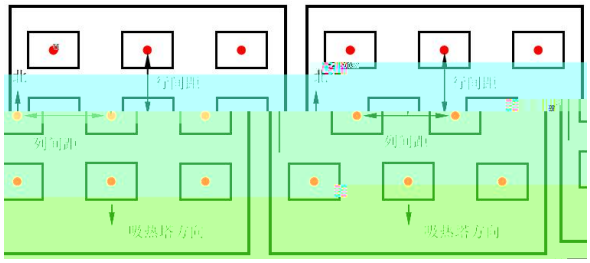

(a) (b)

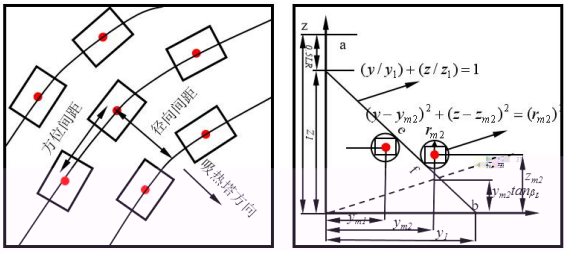

(c) (b)

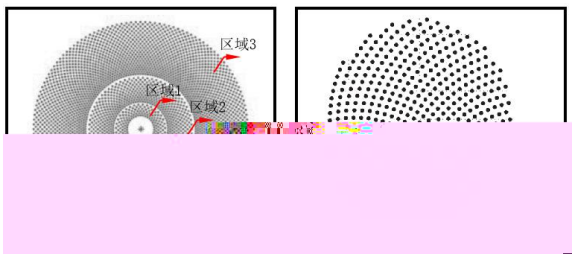

(e) (f)

4

[20]

[21]

[22]

[23]

$$\eta_{i,t}=\rho\,\eta_{cosw}\,\eta_{at}\,\eta_{int}\,\eta_{sb} \quad (2)$$

ρ η_{cosw} η_{at} η_{int} η_{sb}

2.3.1

[24]

1 5a 3

[25]

[26]

[27]

[28]

2 5b

[29,30]

$$\eta_{sb}=1-(N_s+N_b)/(N-N_{grd}) \quad (3)$$

N_s N_b N N_{grd}

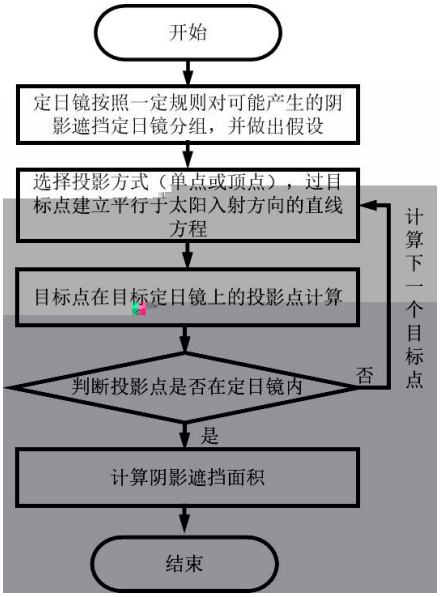

(a)

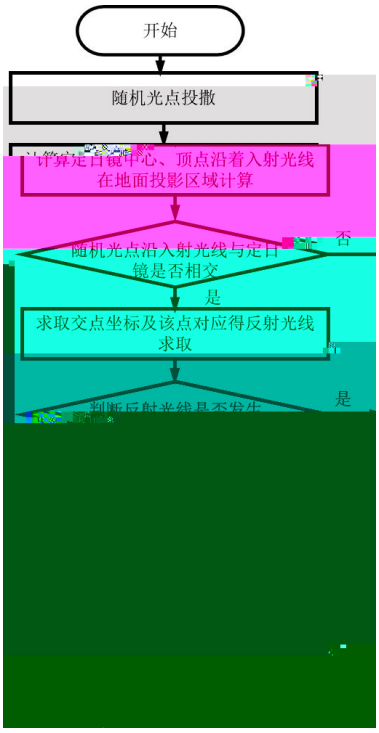

(b) Monte-Carlo

5

2.3.2

[32]

[29]

$$\eta_{\text{int}}=1 \quad N_{\text{int}} / (N \quad N_{\text{grd}} \quad N_{\text{b}}) \qquad 4$$

N_{int}

2.4

Hermitte [5,13] UNIZAR [33]

HFLCAL [10]

DELSOL3 SolarPilot

Hermitte

[13]

$$F \quad x,y \quad \frac{1}{2 \quad x \quad y}\exp[\quad \frac{1}{2}(\frac{x}{x})^2 \quad \frac{1}{2}(\frac{y}{y})^2] \cdot \sum_{i=0}^{I} \sum_{j=0}^{J} A_{i,j} H_i(\frac{x}{x}) H_j(\frac{y}{y}) \frac{1}{i!\,j!} \qquad (5)$$

5 Hermitte

Hermitte

$H_i(x)$ H_j y $A_{i,j}$

[33] UNIZAR

HFLCAL

[34] UNIZAR HFLCAL

[36]

594

[41]

[9] WEI X, Lu Z , Lin Z ,et al. Optimization procedure for design of heliostat field layout of a 1MWe solar tower thermal power plant[C]. Solid State Lighting & Solar Energy Technologies. 2007

[10] SCHWARZBZL P , PITZ-PAAL R , Schmitz M. Visual HFLCAL-A Software Tool for Layout and Optimisation of Heliostat Fields[C]. Solarpaces. DLR, 2009.M. Izygon

[11] P. Armstrong, C. Nilsson, N. Vu, TieSOL–A GPU-BasedSuite of Software for Central Receiver Solar Power Plants[C]. Proceedings of the 2011 SolarPACES International Symposium, Granada, Spain,2011

[12] COLLADO F J, GUALLAR J. Campo: Generation of regular heliostat fields[J]. Renewable Energy, 2012, 46:49-59

[13] WAGNER M J, WENDELIN T. SolarPILOT: A power tower solar field layout and characterization tool[J]. Solar Energy 2018,171:185-196

[14] [M]. , 2019:67-77

[15] SMUTUBERRIA A, PASCAL J, GUISADO M, et al. Comparison of heliostat field layout design metholofies and impact on power plant efficiency[J]. Energy Procedia2015, 69:1360-1370

[16] M.D. Walzel, LIPPS F W, VANT-Hull L L. A solar flux density calculation for a solar tower concentrator using a two-dimensional hermite function expansion[J]. Solar Energy, 1977, 19(3):239-253

[17] SIALA F, MEE F. Mathematical formulation of a graphical method for a no-blocking heliostat field layout[J]. Renewable Energy, 2001, 23(1):77-92

[18] NOONE C J, TORRILHON M, MITSOS A. Heliostat field optimization: A new computationally efficient model and biomimetic layout[J]. Solar Energy, 2012, 86(2):792-803

[19] ZHANG M, Du X, YANG L, et al. Comparing study of biomimetic spiral and radial staggered layouts of the heliostat field[J]. Energy Procedia, 2015, 69:242-249

[20] ALDULAIMI R, MS Söylemez. Performance analysis of multilevel heliostat hield layout[J]. Turkish Journal of Science & Technology, 2016,11(2):11-20

[21] SAGHAFIFAR M, GADALLA M, MOHAMMADI K. Thermo-economic analysis and optimization of heliostat fields using AINEH code: Analysis of implementation of non-equal heliostats (AINEH)[J]. Renewable Energy, 2019,135:920-935

[22] [J]. ,2018(2):64-66+70

[23] SCHMITZ M, SCHWARZBZL P, BUCK R, et al. Assessment of the potential improvement due to multiple apertures in central receiver systems with secondary concentrators[J]. Solar Energy, 2006, 80(1):111-120

[24] HUANG W, LI L, LI Y, et al. Development and evaluation of several models for precise and fast calculations of shading and blocking in heliostats field[J]. Solar Energy, 2013, 95:255-264

[25] LIPPS F W, VANRHULL L L. Shading and blocking geometry for a solar tower concentrator with rectangular mirrors [J]. American Society of Mechanical Engineers, 1974, 1(4): 57-58

[26] VITTITOE C N, BIGGS F.The HELIOS model for the optical behavior of reflecting solar concentrators[R]. Albuquerque USA, Sandia National Laboratory,1976

[27] McFee, R.H. Computer program concen for calculation of irradiation of solar power central receiver[C]. ERDA Workshop on Methods for Optical Analysis of Central Receiver Systems, Universityof Houston,1974

[28] SASSI G. Some notes on shadow and blockage effects[J]. Solar Energy, 1983, 31(3):331-333

[29] [D] : , 2014:26-34

[30] SANCHEZ M , ROMERO M. Methodology for generation of heliostat field layout in central receiver systems based on yearly normalized energy surfaces[J]. Solar Energy, 2006, 80(7):861-874

[31] SALOMÉ A, CHHEL F , FLAMANT G , et al. Control of the flux distribution on a solar tower receiver using an optimized aiming point strategy: Application to THEMIS solar tower[J]. Solar Energy, 2013, 94(aug.):352-366

[32] LIPPS F W , WALZEL M D. An analytic evaluation of the flux density due to sunlight reflected from a flat mirror having a polygonal boundary[J]. Solar Energy, 1978, 21(2):113-121

[33] COLLADO F J , GÓMEZ A, TURÉGANO J A. An anaanalytic function for the flux density due to sunlight reflected from a heliostat[J]. Solar Energy, 1986, 37(3):215-234

[34] COLLADO, F J. One-point fitting of the flux density produced by a heliostat[J]. Solar Energy, 2010, 84(4): 673-684

[35] WANG J, DUAN L, YANG Y. Rapid design of a heliostat field by analytic geometry methods and evaluation of maximum optical efficiency map[J]. Solar Energy, 2019,180:456-467

[36] CARRIZOSA.E,DOMINGGUEZ-BRAVO.C,FERNAN-DEZ-CARA E et al. A heuristic method for simultaneous tower and pattern-free field optimization on solar power systems[J]. Computers & Operations Research, 2015, 57(C):109-122

[37] COLLADO, F J., GUALLAR, J. Two-stages optimised design of the collector field of solar power tower plants[J]. Solar Energy, 2016, 135:884-896

[38] COFARGES O, BEZIAN J J., ELHafi M. Global optimization of solar power tower systems using a Monte Carlo algorithm: Application to a redesign of the PS10 solar thermal power plant[J]. Renewwable Energy 2018,119:345-353

[39] CHAO L, ZhAI R, LIU H, et al. Optimization of a heliostat field layout using hybrid PSO-GA algorithm[J]. Applied Thermal Engineering, 2018, 128:33-41

1 1 1 2 1

/ 3 / . . / + . . 0 . 0 1 . 0 + . . 2 + . 3

Desing and Implementation of Energy Management System for Industrial Park-used Photovolatic-energy Storage-charging System

WANG Zhimin LIN Yunsong YAN Zhiguo ZHANG Chuan ZHANG Haoheng

& / , , , / . . . 0 , & '

, , / / 1 /

Abstract: Based on the research of photovoltaic-energy storage-charging system, an industrial park-used energy management system was designed. The software architecture and the function design including device management system management data presentation energy analysis of the energy management system were introduced. Based on the energy generated by the photovoltaic system, the load and the peak-valley electricity time distribution, an energy management strategy was made, and the maximal economic profits was achieved.

Key words: photovolatic-energy storage-charging system; energy storage; energy management system

/ +0

2 . .

0 . 0 1 +. 1 +0 .

/ .

/

/

0

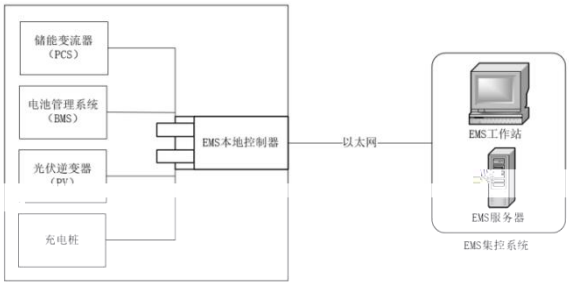

0

0 , /

1 +2

1

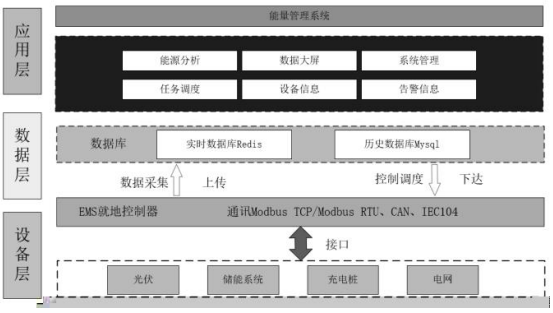

1

0 , 0

2

0 1 0 2 3

/ . 2

2

y

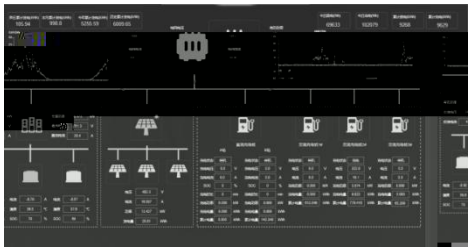

3 +

1 ，2

/

/

1 ，3

/ 0 . . / 0 . .

/ . . 1

/ 2 . . 0 / . .

. . / / . .

0 / 0 . . / 2 . . . ,3 0

0 / . . 0 1 . .

1 0 1 . . . . . ,0 /

/ .

/ .

/

. #

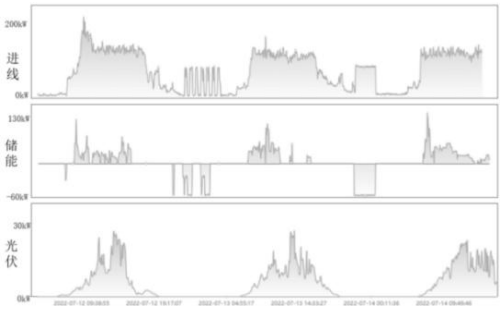
进线
储能
光伏

SolidWorks

1.2

3

4

5

0 ɔ ﴾ ⅞ ’ ㅓX

2.1

AutoCAD

1 ε ʐ ᶊ

3.1

A

1

2.2

SolidWorks

[3]

SolidWorks

“ ” “ ”

1

2

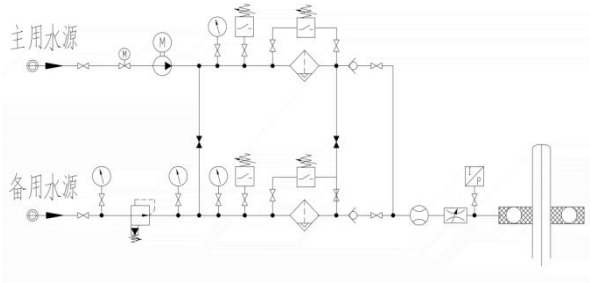

1 A

3.2

1

4.2

“ ”

[5]

1 “ ”
“
”

2
“ ”

4.3

1

2

3

2 Qmjgb Umpiq ﻮﺋ ⅞ ’

4.1

“ ”

[4]

2

2

“ ” 3

3

5

6

4.4

[6]

Solidworks

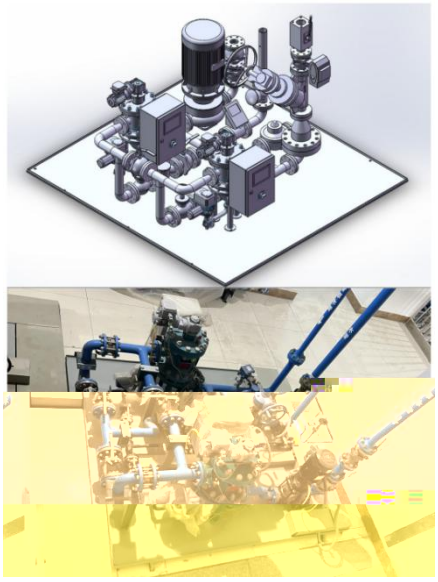

6 B

4

4.5

4 Solidworks

7

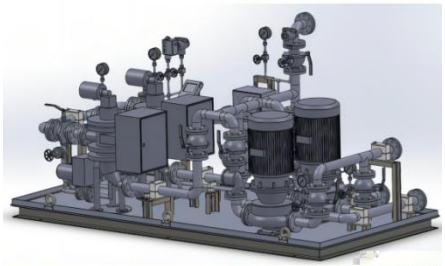

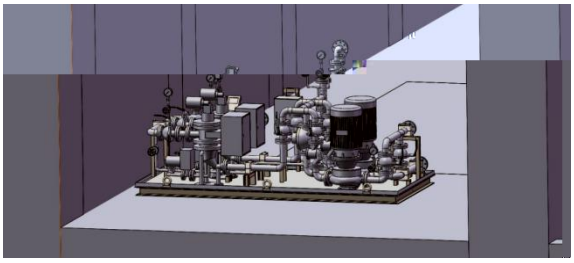

5 A

7

3

618000

Installation Process of Integral Yoke Ring for High Head Suspended Pumped Storage Unit

ZHANG Xiang YANG Yuewei

Abstract: The integral yoke ring structure yoke has the advantages of good rigidity and short installation period, and is applied more and more popular. In this paper, the structure of integral yoke ring of high head suspended pumped storage unit is introduced, the technical difficulties of integral yoke installation process are analyzed in detail, and the problems of yoke lifting, size adjustment and measurement, quality control of hot-key and so on are solved.

Key words: pumped storage unit; integral yoke ring; suspension generator; installation process

1

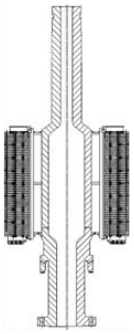

2

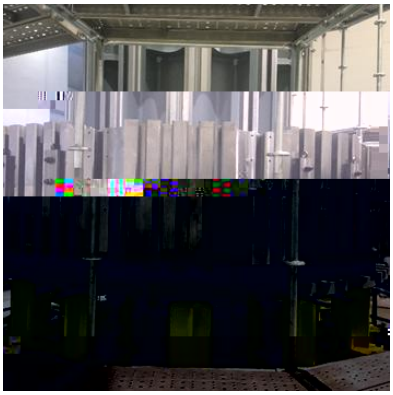

3

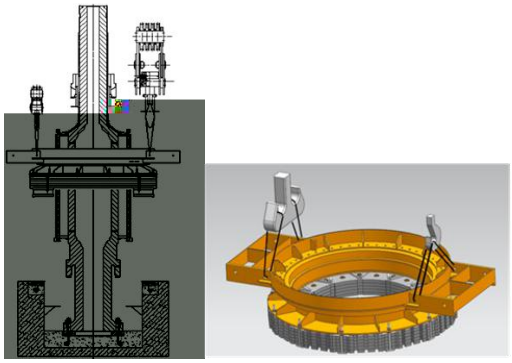

60 %

5

3.4

+

5

4

56

[1] . [M]. , 2008.6
[2] GB/T 8564-2003, [S]
[3] DL/T 5230-2009, [S]
. 2008 (3):80-82+149
[2] , , . [J]. , 2018 (2):95-99+159
[3] , , . SolidWorks BIM [J]. , 2022, 50(4):79-83
[4] . SolidWorks [J]. . 2022, 12 (7):88-90
[5] , , . [J]. , 2018, 8(4):104-106
[6] . [J]. , 2014 (4) : 58-62
[1] . [J].

1,2 2 3 3 1,2 2 1,2 3

1. 611731 2. 611731;
3. 250200

-

X703.1 A 1001-9006 2023 02-0061-06

Techno-economic Analysis on Design of Oxidation Air Blowers for High Sulfur Coal Limestone Wet Flue Gas Desulfurization

YANG Zhizhong[1,2], *LV Lidan*[2]

1

n

m

1.1 [2-4]

-

SO_2 $CaCO_3$

$CaSO_4 \cdot 2H_2O$ 1

$CaCO_3+SO_2+1/2O_2+2H_2O \rightarrow CaSO_4 \cdot 2H_2O \downarrow +CO_2 \uparrow$ 1

2

$$Q=\frac{0.5\times 22.4\times Q_{gas}C_{SO_2}\times\eta\times(1-\alpha)}{64\times 0.21\times 10^6\beta}$$ 2

2

Q Nm^3/h

0.5

22.4 $m^3/kmol$

Q_{gas}— Nm^3/h

C_{SO_2}— SO_2 mg/Nm^3

η SO_2

α SO_2

0.2

β

0.3~0.4

64 SO_2

0.21

2.2

$P=P1+P2$ 3

3

P kPa 5 % 10 %

$P1$ kPa

$P2$ kPa

$P1=\rho gh\times 10^{-3}$ 4

2

-

[5]

1

2

2 980 / 3 550 / +

100 20

dB(A)

68 %

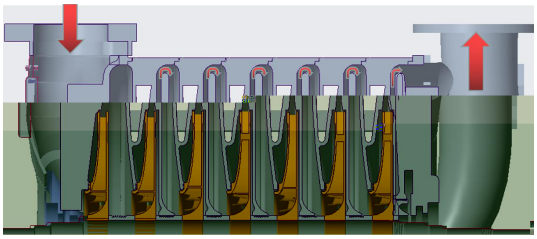

2

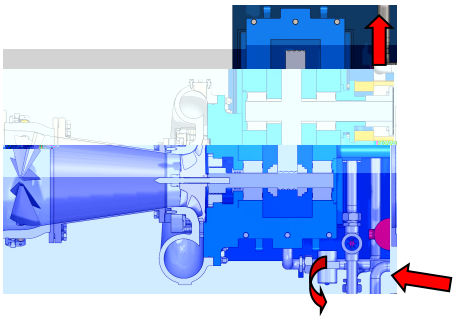

3

3

2

+

3

4

+PLC

8 000 30 000 /

40 % 105 %

70 % 77 %

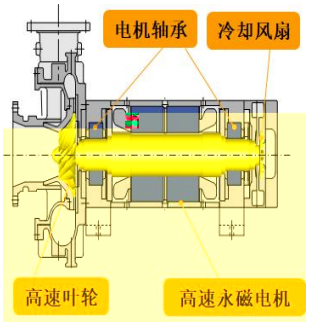

4

4

[6] 5

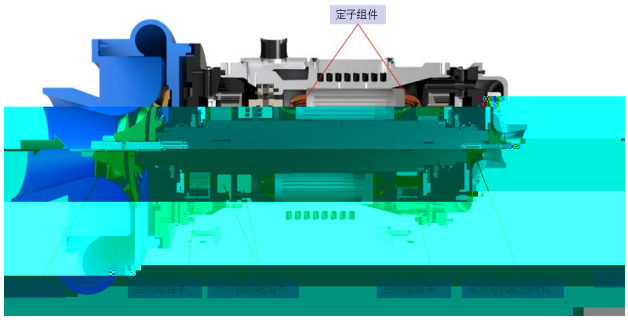

PLC

5

5

1

1

m^3/min	≤ 1 400	≤ 2 000	≤ 2 000	≤ 600	≤ 600
kPa	≤ 98 / ≤ 196	≤ 145	≤ 196	≤ 120	≤ 150
%	64~70	70~78	≥ 83	85	85
dB A	≥ 100	85~100	90~95	80	80
	1~2	3~5	≥ 10	3~5	
	5~8	10	20	20	20
r/min	700~1 500	3 000~3 550	8 000~35 000		
%	90~95	90~95	90~97	≥ 95	≥ 97

r/min	1 400~3 000	2 980/3 550	/		
			1 400~35 000		60 000
%	57	61~68	65~70	70~75	77

3

+

14 18 m

160 kPa

+

6

+

98 kPa

+

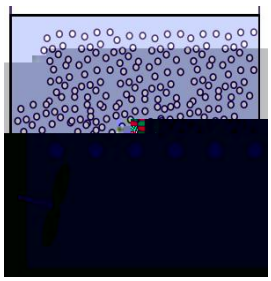

A

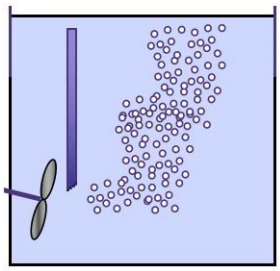

B

6

4

660 MW

10.2 794.4 hPa 79%

197.4 × 104 Nm³/h 6.16 %

4.92 % SO_2 9 000 mg/Nm³ 6 %O_2

- SO_2

≤ 35 mg/Nm³ 6 %O_2

34 568 Nm³/h

88.2 kPa

N+1 N 1

98 kPa

3

2

Nm³/h	34 568	34 568	34 568	34 568	34 568
	3+1	2+1	2+1	3+1	3+1
Nm³/h	11 523	17 284	17 284	11 523	11 523

m^3/h	15 760	23 640	23 640	15 760	15 760
kPa	79.44	79.44	79.44	79.44	79.44
kPa	88.2	88.2	88.2	88.2	88.2
%	65	70	80	85	85
kW	472.9	650.6	558	347.3	347.3
%	57	61	68	72	77
kW	543.6	747.8	656.5	408.6	385.9
kW	630	800	710	450	425
kW	1 631	1 496	1 313	1 226	1 158
	230	280	320	300	300
	4	3	3		
	4	3	3		
	652.4	598.4	525.2	480.4	463.2
	882.4	878.4	845.2	780.4	763.2

1.

2.

3. 8 000 h kW · h 0.50

4.

98 kPa

4

5

1

2

3

+

[1] DL/T 5196-2016, - [S]

[2] . - [D]. : , 2009

[3] , , . [J] . , 2018,37(3):86-88

[4] , , . [J]. , 2021(5):52-54

[5] . [J]. , 2013(12):88-89

[6] . [J]. , 2014, 40(13):142-143

618000

Coupling Calculation of Flow and Heat Transfer in Different Rotor end Structures of High-speed Hidden Pole Motor

YANG Yan WANG Chao ZHOU Guanghou

Abstract: This paper describes the rotor flow characteristics and heat transfer characteristics of high-speed hidden pole motor under different rotor end cooling structures. For a large-scale highspeed hidden pole motor, the three-dimensional flow field and temperature field of the motor during steady-state operation are solved by the finite volume method. The influence of the rotor end ventilation structure on the characteristics of the rotor flow field and temperature field is studied. The flow distribution of each rotor duct, the static pressure distribution of the rotor duct, the heat dissipation coefficient and temperature rise distribution of the rotor ventilation duct under different rotor end structures are analyzed and obtained. The research results understanding the characteristics of rotor ventilation structure of similar motors further, and are reference for more ventilation structure design of high-speed hidden pole motor in the future.

Key words: high-speed hidden pole motor; rotor end cooling structure; computational fluid dynamics; coupling calculation

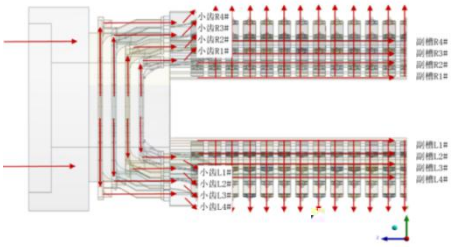

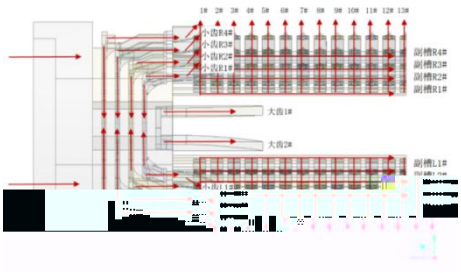

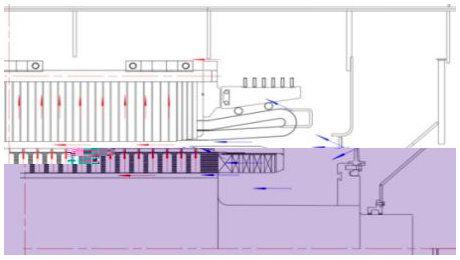

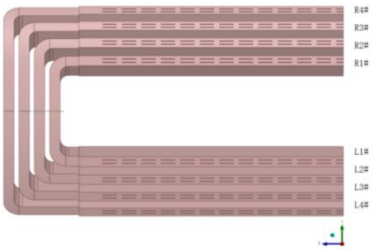

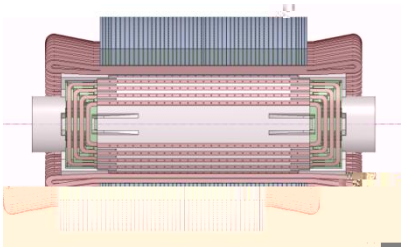

$\frac{}{t}$ u

t u

$\frac{u}{t}$ F p — u u

F p

μ

κ-ε

$\frac{}{t}$ div V div $grad$ S

V Γ S

uT $gardT$ S.

u Γ

$$\frac{\partial}{\partial x}\left(k_x \frac{\partial T}{\partial x}\right)+\frac{\partial}{\partial y}\left(k_y \frac{\partial T}{\partial y}\right)+\frac{\partial}{\partial z}\left(k_z \frac{\partial T}{\partial z}\right)=-q$$

k k k

· T q

$\eta = \frac{Q}{Q}$

Q Q

$_i$ $_i$ i N

$p_{s\,i}$ $p_{d\,i}$ $p_{s\,i}$ $p_{d\,i}$ p_{i} $_i$ i N

$p_{s\,i}$ $_i$ $p_{s\,i}$ $p_{s\,i}$ — $_i$ — $_i$ $\frac{L}{D}$— $_i$ i N

“ ”

P_s P_d

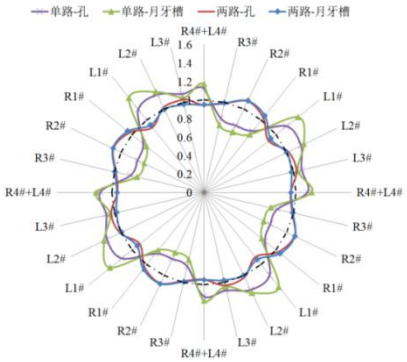

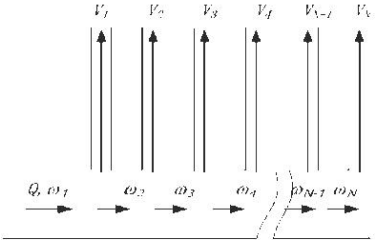

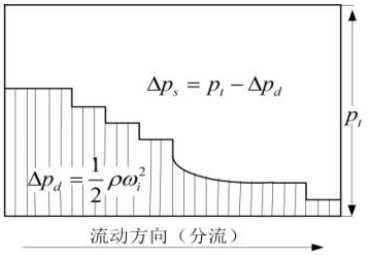

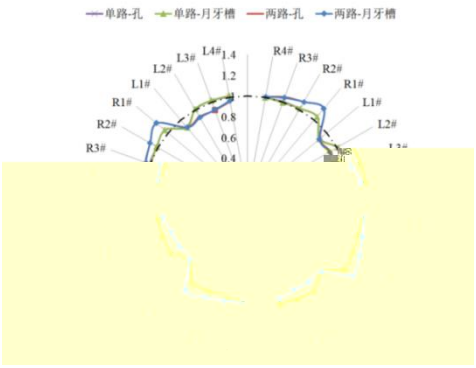

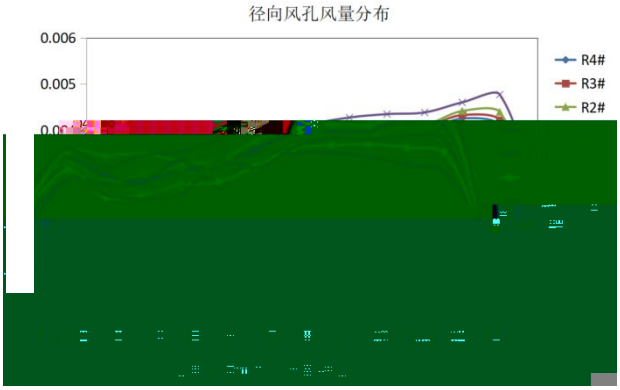

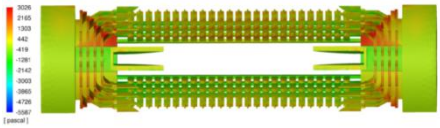

$$\eta_\alpha = \frac{\alpha_i}{(\quad \text{or} \quad)}$$

α_i i

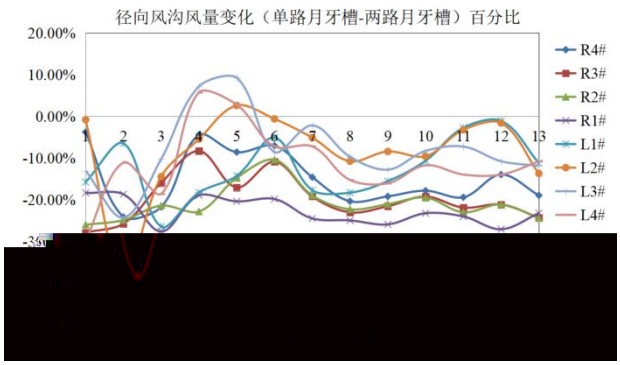

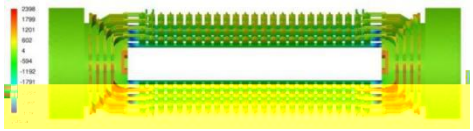

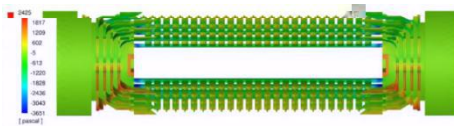

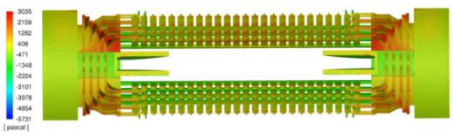

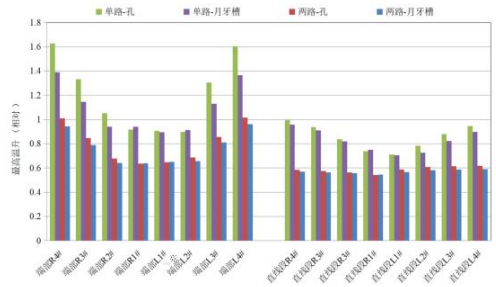

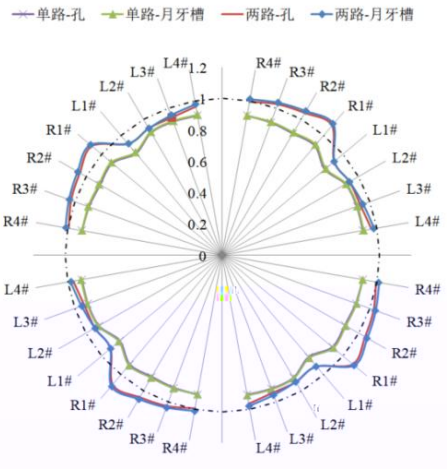

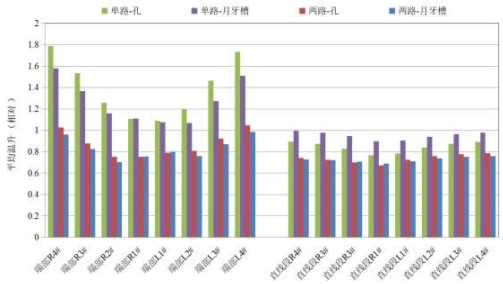

$$\eta = \frac{\Delta T_i}{}$$

ΔT_i i

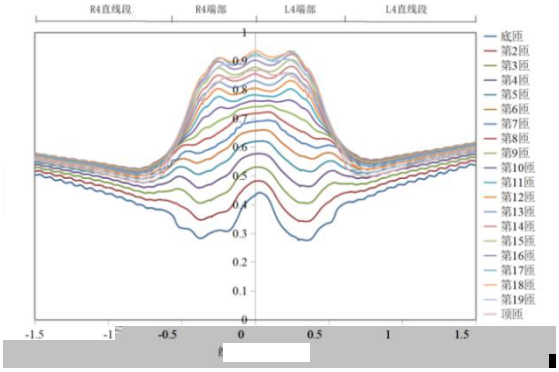
R4直线段
R4端部
L4端部
L4直线段
底匝
第2匝
第3匝
第4匝
第5匝
第6匝
第7匝
第8匝
第9匝
第10匝
第11匝
第12匝
第13匝
第14匝
第15匝
第16匝
第17匝
第18匝
第19匝
顶匝

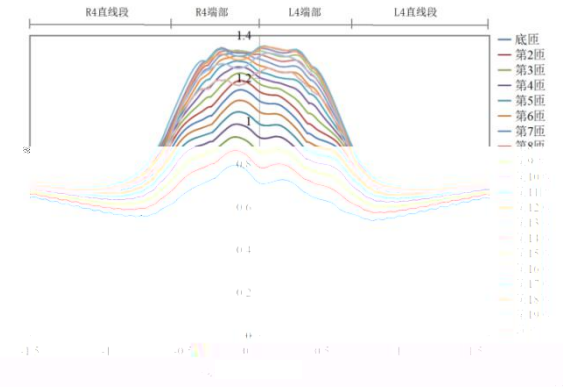
R4直线段
R4端部
L4端部
L4直线段
底匝
第2匝
第3匝
第4匝
第5匝
第6匝
第7匝

611731

D

S S

Z

Z

1

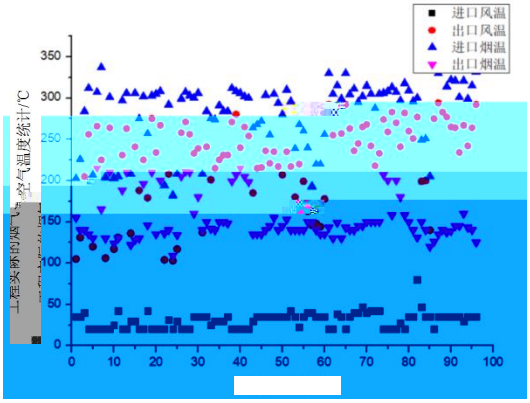

$$h_g = 0.023\frac{\lambda}{De}(\frac{\omega De}{\nu})^{0.8}Pr^{0.3}C_k \quad (1)$$

$$h_a = 0.36C_S\frac{\lambda}{De}(\frac{\omega De}{\nu})^{0.6}Pr^{0.33} \quad (2)$$

$$C_{fg} = C_z(\frac{\omega De}{\nu})^{-0.27} \quad (3)$$

$$C_{fa} = (1.82\log(\frac{\omega De}{\nu}) - 1.64)^{-2} \quad (4)$$

h_g h

λ

D ω

ν Pr

C

C C

C C

P D L V ρ

k-ε

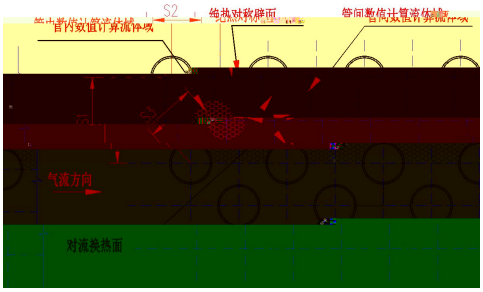

k ε

h

C

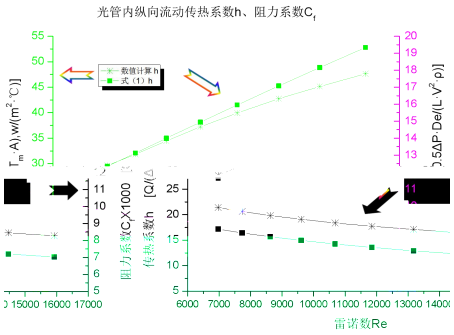

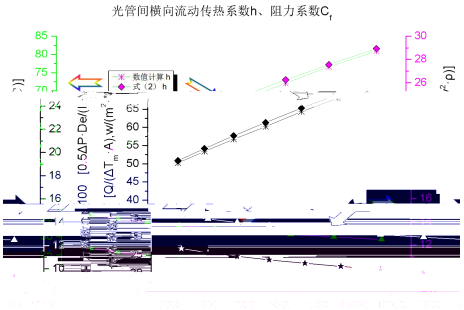

h

C

2

D

P W

H

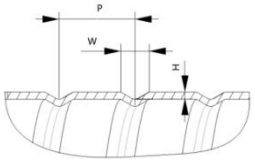

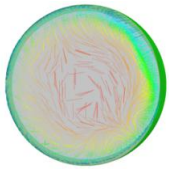
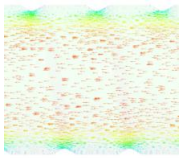
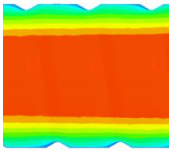
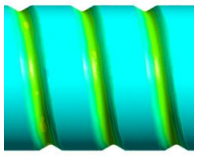

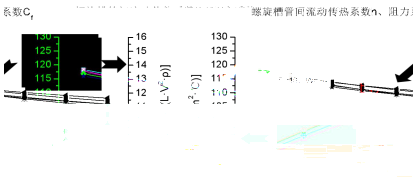

螺旋槽管内流动传热系数h、阻力系数C_f

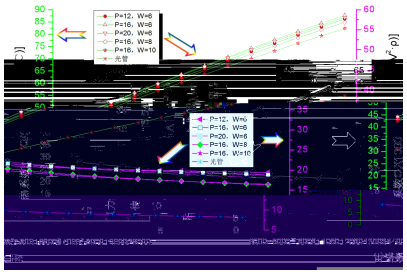

k-ε

h C

W

P

P P

k-ε

P

h C

W

W

P

P

P P

P

P P

W

W

W

W

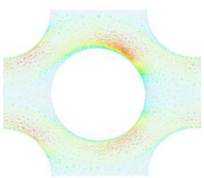
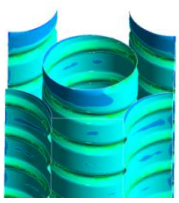

3

Q N

N C

P NTU

O E N

O R

L N E

$$EI = Q - N$$

O

E N

R

L

N

C G

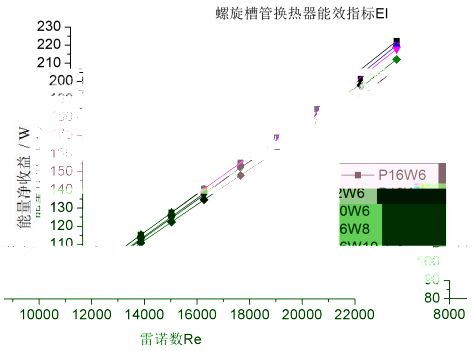

с и

4

628000

127 km

0.1 h 2.4h 4h

TM75 A 1001-9006 2023 02-0085-04

Research and Application of Remote Automation System for High Voltage Transmission Line in Yuanba Gas Field

YANG Yang, *ZHANG Wen*, *LI Changchun*, *JIANG Yufeng*, *BI Quanyun*, *ZHANG Yongtao*

(Guangyuan Natural Gas Purification Company of Sinopec Southwest Oil and Gas Company, 628000, Guangyuan, Sichuan, China)

Abstract: Yuanba Gas Field is the second super-deep marine gas field deployed by Sinopec in the Sichuan Basin, located in the northeast mountain area of Sichuan Province. The high-voltage transmission line of Yuanba Gas Field is the only source of power of Yuanba Gas Field, with a total length of about 127 km. The transmission line is characterized by wide distribution, bad natural environment, and difficulty in troubleshooting. In combination with the actual situation of the high voltage transmission line in Yuanba Gas Field, in order to solve the problem of troubleshooting the high voltage transmission line, shorten the troubleshooting and processing time, and reduce the labor cost, a set of remote automation system for the high voltage transmission line has been developed from the aspects of software, hardware, and ligand system. The average time for the system to automatically process the fault is 0.1 h. The system shows that the average time for manual processing of fault points is 2.4 hours, which is far better than the previous average time for manual troubleshooting and processing of fault points, and it has important research and application value.

Key words: high voltage; transmission line; long-range; automation; failure point

1 460

10 kV 10 kV

[1] 10kV 127 km

47

[2-3]

2023-02-21

1992— , 2018

[4]

10 kV

[2,5,6]

10 kV

(FTU) [7-8]

FTU

FTU

GPRS+SIM

[9]

[10-11]

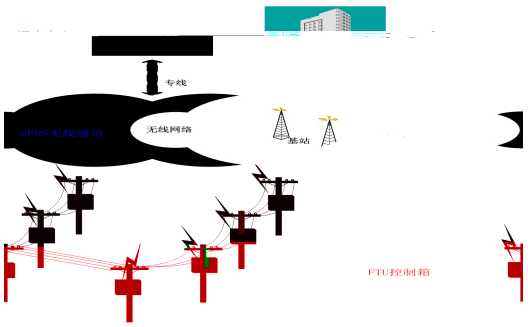

1

2.1

FTU SIM

10 kV

SL200e SL200e

2.2

2

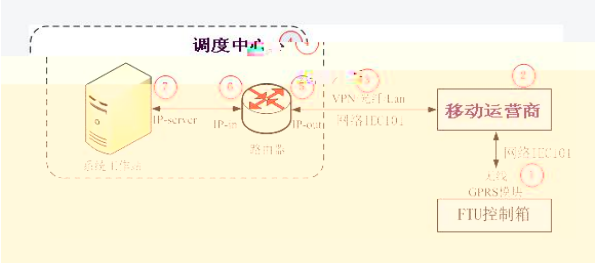

2

1

GPRS IP port

GPRS IP port 5 IP-out +

port 2 IEC101

FTU client server

client server socket 3

VPN/ /Lan 10 kV

VPN VPN

“ Virtual Private Network ” “

”

Internet

4

IP FTU

5

IP port

6

IP IP-in

IP IP-server

7 IP IP-server 10

port IP kV

IP 8 IP-server

FTU

socket 4 0.1

2.3

FTU IP

VPN

10 kV

FTU

GPRS+SIM

3

2.4

10 kV

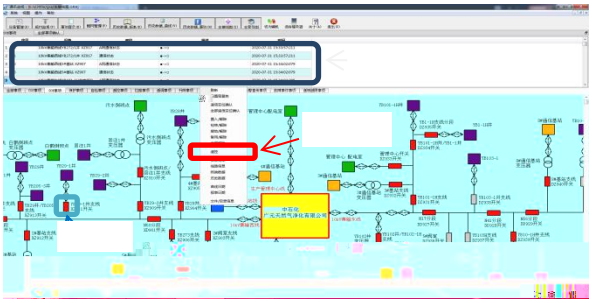

3 10kV

1 2021 4 8

				h
10 kV	G906 “ ” “ ”			0.1
10 kV	G904 “ ” “ ”		0.4kV	0.5
10 kV	YB1-1H DZ935 “ ”			0.1
10 kV	YB27-3 XZ919 “ ”			1
10 kV	YB1-1H DZ935 “ ”			0.1
10 kV	YB205 XZ915 “ ” XZ916			0.1
10 kV	YB27-3 XZ919 “ ”			1
10 kV	6# NZ949 “ ”			0.1
10 kV	YB103-1			0.8
10 kV	YB29-2 XZ909 “ ”			0.6
10 kV	YB27-1/2 XZ923 “ ”			0.1
10 kV	YB29-1 XZ911 “ ”			0.8
10 kV	2# XZ912 “ ”			0.1

( )

2021 4

8 1 10 kV

13

7

0.1

0.8 h

4 h

2 2021

h
4
2.4
0.1

2 2021

4 h 2.4 h

0.1 h

10kV

0.1 h

2.4 h

4 h

[1] , , .
[J]. , 2022, (8):74-77

[2] . DSP
[D]. , 2004

[3] , , .
[P]. CN112505488B,2023-05-26

[4] . [J].
, 2021 (23):97-98

[5] , , .
[J]. , 2010, (3):29-32

[6] . 10kV [J]. ,
2004, 18(3):141-146+150

[7] , . 220kV [J].
, 2022 (16):38-41

[8] .
[D]. , 2007

[9] , , . GPRS
[J]. , 2015, 29(1):9-14

[10] , , . ARM FTU
[J]. , 2014, (10):62-63

[11] , , .
[J]. , 2022(4):83-85+88